BBA - General Subjects 1863 (2019) 1098–1107

Contents lists available at ScienceDirect

BBA - General Subjects

journal homepage: www.elsevier.com/locate/bbagen

Multicolor redox sensor proteins can visualize redox changes in various compartments of the living cell

Kazunori Sugiura[a,b], Hideaki Tanaka[c], Genji Kurisu[c], Ken-ichi Wakabayashi[a], Toru Hisabori[a,b,*]

[a] Laboratory for Chemistry and Life Science, Institute of Innovative Research, Tokyo Institute of Technology, Nagatsuta-cho 4259, Midori-ku, Yokohama 226-8503, Japan
[b] Core Research for Evolutional Science and Technology (CREST), Japan Science and Technology Agency (JST), Chiyoda-Ku, Tokyo 102-0076, Japan
[c] Laboratory of Protein Crystallography, Institute for Protein Research, Osaka University, Yamadaoka 3-2, Suita, Osaka 565-0871, Japan

ARTICLE INFO

Keywords:
Biosensor
Fluorescence
Fluorescence lifetime
Protein design

ABSTRACT

Change in the intracellular redox state is a consequence of various metabolic reactions, which simultaneously regulates various physiological phenomena in cells. Monitoring the redox state in living cells is thus very important for understanding cellular physiology. Various genetically encoded fluorescent redox sensors have therefore been developed. Recently, we developed oxidation-sensitive fluorescent proteins named Oba-Q (Sugiura, K., et al. (2015) *Biochem. Biophys. Res. Commun.* 457, 242–248), which exhibit dramatic quenching under oxidizing conditions. To extend the range of uses of redox sensor proteins, we refined these proteins based on the molecular architecture applied to Oba-Q, and successfully produced several redox sensor proteins based on CFP and YFP. Interestingly, some of these sensor proteins showed the reverse changes in emission compared with Oba-Q, implying remarkable fluorescence quenching under reducing conditions. We named this type of sensor protein Re-Q, reduction-sensed quenching protein. The cause of the redox-dependent fluorescence quenching could be clearly explained based on the crystal structure of Re-Q in the reduced and oxidized forms. In addition, by introducing suitable mutations into the sensors, we produced Oba-Q and Re-Q mutants exhibiting various midpoint redox potentials. This series of proteins can cover a wide range of redox potentials in the cell, so they should be applicable to various cells and even intracellular organelles. As an example, we successfully measured the redox responses in different cell compartments of cultured mammalian cells simultaneously against the anticancer reagents Kp372-1.

1. Introduction

Redox balance affects the viability of cells via changes in various enzyme activities caused by oxidation or reduction of the enzyme molecules, and changes in various macromolecular conditions in the cells. For example, reactive oxygen species (ROS) are readily produced as a consequence of the sensing of electrons by oxygen molecules in vivo [1]. ROS are toxic in cells because they can vigorously oxidize various bio-macromolecules such as proteins, nucleic acids, and lipids; however, at low levels ROS work as critical signaling molecules in some cases. For instance, the accumulation of ROS in mitochondria induces programmed cell death [2]. In plants, excess light induces the production of ROS [3], which cause intense damage to the whole body of the plant. Redox balance in the cell is also a key factor in controlling various cellular activities, and thioredoxin (Trx) has a significant role as an intracellular redox mediator protein [4]. In addition, peroxiredoxin (Prx) [5] [6], major significant protein that uses the Trx-mediated reducing power, functions for the detoxification of ROS in various cells. Hence, the supply and usage of reducing power in cells are critical for the total range of cellular activities, so the redox balance in the cell must be maintained at a certain level irrespective of changes in the extracellular environment. This mechanism is referred to as redox homeostasis [7,8].

To study intracellular redox homeostasis, direct monitoring of the redox state in the cell should provide us with valuable information. For this purpose, various redox-sensitive fluorescent sensor proteins such as redox-sensitive green fluorescent protein (roGFP) [9], rxYFP [10], Redoxfluor [11], and rxRFP [12] have been developed. roGFP was

Abbreviations: CFP, cyan fluorescent protein; FRET, Förster resonance energy transfer; Oba-Q, oxidation balance-sensed quenching protein; Prx, peroxiredoxin; ROS, reactive oxygen species; RFP, red fluorescent protein; roGFP, redox-sensitive green fluorescent protein; Re-Q protein, reduction-sensed quenching protein; Trx, thioredoxin; YFP, yellow fluorescent protein.

* Corresponding author at: Laboratory for Chemistry and Life Science, Tokyo Institute of Technology, Nagatsuta 4259-R1-8, Midori-ku, Yokohama 226-8503, Japan.
E-mail address: thisabor@res.titech.ac.jp (T. Hisabori).

https://doi.org/10.1016/j.bbagen.2019.01.016
Received 29 November 2018; Received in revised form 10 January 2019; Accepted 24 January 2019
Available online 04 April 2019

developed by introducing two cysteine residues at positions Ser^{147} and Gln^{204} of the wild-type GFP or GFP_{S65T} mutant; they were named roGFP1 and roGFP2, respectively [9]. These two cysteine residues are sufficiently close to each other to form a disulfide bond under oxidizing conditions. The roGFP proteins have two fluorescence excitation peaks at around 400 and 490 nm, and the ratio of fluorescence intensities of these two peaks changes according to the formation and dissociation of the disulfide bond. rxYFP is also a popular redox sensor protein, which is produced by substituting Asn^{149} and Ser^{202} of yellow fluorescent protein (YFP) with cysteines [10]. rxYFP has a single excitation peak at 512 nm and the fluorescence intensity is affected by the formation of a disulfide bond in the protein molecule. Midpoint redox potentials of roGFP1, roGFP2, and rxYFP were reported to be −287, −272, and − 262 mV, respectively [9,10]. Lohaman and Remington succeeded in creating roGFP1 mutants with higher midpoint redox potential by introducing a single amino acid insertion at the C-terminal side of Cys^{147} and the substitution of His^{148} to Ser [13]. These mutants were named roGFP insertion X (roGFPiX, where X is the single-character code of the inserted amino acid), and they showed higher midpoint redox potential at around −229 to −246 mV. As a redox sensor protein having an emission peak at the longer-wavelength region, rxRFP was derived from the red fluorescent protein (RFP) [12]. Redoxfluor is a redox sensor protein based on the Förster resonance energy transfer (FRET) between cyan fluorescent protein (CFP) and YFP [11]. The efficiency of FRET was affected by environmental redox conditions caused by the conformational change of the cysteine-containing linker region between CFP and YFP [11].

Recently, we developed several redox sensor proteins based on CFP and Sirius, the GFP variant having the shortest emission wavelength [14], by the introduction of two cysteine residues at the same positions as roGFP together with insertion of an amino acid at the C-terminal side of Cys^{147} and introduction of a single mutation at position 146 [15]. Interestingly, our redox sensor proteins showed rapid quenching of their fluorescence under oxidizing conditions, so we named them Oba-Q (oxidation balance-sensed quenching proteins) [15].

Though the Oba-Q proteins have several advantages over the other redox sensors such as rapid response and pH stability, they also have some disadvantages (for details, see Comini 2016). For example, midpoint redox potentials of the Oba-Q proteins are too high to use them in a reducing microenvironment, such as the mitochondrial matrix ($E_{pH=8}$ ∼ −360 mV) [9] and cytoplasm ($E_{pH=7}$ ∼ −320 mV) [16] of HeLa cells.

We therefore attempted to improve the redox sensor proteins to make them applicable to various organelles in cells as well as to make them useful as a multicolor visualization system. By using a strategy referring from the development of Oba-Q, we successfully obtained attractive redox sensor proteins, which showed the reverse change in fluorescence from Oba-Q, implying remarkable quenching of the fluorescence under reducing conditions. We named them Re-Q proteins (reduction-sensed quenching proteins). In addition, we obtained several derivative proteins having different midpoint redox potentials, which can cover the wide range of possible redox potentials in the various compartments in the cell. Crystal structure analysis of our newly developed redox sensor protein in two different redox states revealed the molecular mechanism by which the protein shows the remarkable change in fluorescence dependent on the formation and dissociation of disulfide bonds.

2. Experimental procedures

2.1. Gene construction, mutagenesis, and protein expression/purification

To obtain Oba-Q and Re-Q mutants, genes for CFP', the variant of mTurquoise with an introduced L46F mutation and Venus in pET23a were used as a template, and all of the point mutations and initial insertions were introduced into the desired genes using PrimeSTAR® Mutagenesis Basal Kit (Takara). All Oba-Q and Re-Q mutants in pET23a were expressed in *E. coli* strain BL21 by allowing cultures to reach an OD_{600} of between 0.4 and 0.8 at 37 °C, and then the temperature was reduced to 21 °C overnight in the presence of a final concentration of 1 mM IPTG.

Cells were disrupted by French press, and cell lysate was heated at 60 °C for 10 min to denature contaminating proteins derived from *E. coli* and then centrifuged to remove the denatured proteins. For the in vitro assay of the sensor proteins, the supernatant was applied to a TOYOPEARL Butyl 650 (TOSOH) column and eluted by Tris-HCl (pH 8.0) with a reverse ammonium sulfate gradient from 20% to 0%. Peak fractions eluted from the column were then collected, dialyzed to remove ammonium sulfate, and concentrated using Amicon Ultra (Merck Millipore). For X-ray crystal structure analysis, the supernatant was applied to a Ni-NTA affinity column (QIAGEN) and eluted by a buffer containing 100 mM Tris-HCl (pH 8.0) and 250 mM Imidazole. The obtained peak fractions were desalted by dialysis and concentrated. The concentrated samples were further purified using gel filtration chromatography column (Superdex 200, GE).

2.2. Fluorescence spectroscopy

Fluorescence excitation/emission spectra were measured using a fluorescence spectrophotometer, FP-8500 (JASCO, Tokyo, Japan). For the measurement, excitation wavelengths of 435 and 514 nm were used for CFP- and Venus-based mutants, respectively, while the corresponding emission wavelengths were 480 and 525 nm. Absorbance spectra were measured using a spectrophotometer, V-650 (JASCO, Tokyo, Japan).

2.3. Calculation of midpoint redox potentials

Apparent midpoint redox potentials of Oba-Q and Re-Q proteins were determined based on the method described by Hanson et al. [9], as described below. The equilibrium between the oxidized and reduced forms of Re-Q in the presence of DTT is given by Reaction 1.

$$Re - Q_{ox} + DTT_{red} \leftrightarrow Re - Q_{red} + DTT_{ox} \quad \text{(Reaction 1)}$$

To determine the molecular ratio between the oxidized and reduced forms of Re-Q proteins in solution, the protein samples at 1 μM were prepared in 50 mM Tris-HCl (pH 7.0) containing 20 mM DTT (a mixture of oxidized and reduced forms), and incubated for 3 h for equilibration. The fluorescence spectra were then measured at 25 °C. The concentrations of DTT_{red} and DTT_{ox} at the equilibrium state were calculated according to Eqs. 1 and 2, where $[DTT_{red\text{-}i}]$ and $[DTT_{ox\text{-}i}]$ are the initial concentrations of DTT_{red} and DTT_{ox}, respectively, and $[Re\text{-}Q_{ox\text{-}i}]$ is the initial concentration of the oxidized form of Re-Q. R' denotes the fraction of Re-Q proteins that is in the reduced form.

$$[DTT_{red}] = [DTT_{red-i}] - R'[Re{-}Q_{ox-i}] \quad (1)$$

$$[DTT_{ox}] = [DTT_{ox-i}] + R'[Re{-}Q_{ox-i}] \quad (2)$$

Next, the redox potential of the protein was calculated by applying the Nernst equation:

$$E = E'_{0(DTT)} + (RT/nF) \times \ln [DTT_{ox}]/[DTT_{red}] \quad (3)$$

where $E'_{0(DTT)}$ is the biochemist's standard potential of the DTT_{red}/DTT_{ox} couple [−0.33 V, at pH 7 and 25 °C [17]], R is the gas constant ($8.315\,J\,K^{-1}\,mol^{-1}$), T is the absolute temperature (303.15 K), n is the number of transferred electrons (2), and F is the Faraday constant ($9.649 \times 10^4 C\,mol^{-1}$). To determine the fraction of reduced-form Re-Q proteins, fluorescence intensity at 530 nm upon excitation at 514 nm for

Re-Qy and that at 480 nm upon excitation at 430 nm for Re-Qc were denoted by Φ and used for the analysis. Φ_{red} and Φ_{ox} represent fluorescence intensities of fully reduced and fully oxidized forms of Re-Q proteins, respectively. R' was determined by Eq. (4). Concentrations of oxidized and reduced Re-Q in solution ([Re-Q_{ox}] and [Re-Q_{red}]) were then calculated by Eqs. (5) and (6).

$$R' = (\Phi - \Phi_{ox})/(\Phi_{red} - \Phi_{ox}) \quad (4)$$

$$[Re{-}Q_{red}] = R'[Re{-}Q_{ox-i}] \quad (5)$$

$$[Re{-}Q_{ox}] = (1 - R')[Re{-}Q_{ox-i}] \quad (6)$$

Midpoint redox potentials of Re-Q proteins ($E'_{0(Re\text{-}Q)}$) were calculated by Eq. (7):

$$E'_{0(Re-Q)} = E'_{0(DTT)} + (RT/nF) \times ln\alpha [Re{-}Q_{ox}]/[Re{-}Q_{red}] \quad (7)$$

where α is the ratio of the activity coefficients of oxidized and reduced forms of Re-Q. We plotted E on the x-axis and R' on the y-axis, and fitted a curve by using Eq. (8):

$$y = 1/[1 + \exp\{(x - A_1)A_2\}] \quad (8)$$

where A_1 and A_2 are fitting coefficients, and A_1 gives the midpoint redox potential of the protein of interest.

2.4. X-ray crystal structure analysis of Re-Qy1

Purified protein samples were concentrated to 10–15 mg/ml using Amicon Ultra (Merck Millipore). Crystals of ReQy1 and $ReQy1_{CS}$ were obtained by a hanging-drop vapor diffusion method at 293 K. The crystals of ReQy1 were obtained from droplets comprising 1 μl of 10 mg/ml protein sample and 1 μl of reservoir solution containing 50 mM Tris-HCl (pH 7.0), 150 mM NaCl, 0.25 M trilithium citrate, and 14% (*w/v*) PEG3,350. The crystals of $ReQy1_{CS}$ were obtained from droplets comprising 1 μl of 15 mg/ml protein sample and 1 μl of reservoir solution containing 50 mM Tris-HCl (pH 7.0), 150 mM NaCl, and 20%(w/v) PEG3,350. For cryoprotection, crystals were immersed in 20% (*v*/v) glycerol in crystallization buffer and then cooled in liquid nitrogen. X-ray intensity data were collected on BL44XU at SPring-8 (Harima, Hyogo, Japan) using the CCD detector MX-300HE (Rayonix) at cryogenic temperature (100*K*). The diffraction images were processed and scaled using the software package HKL-2000 [18]. The initial-phase angles were determined by the molecular replacement method with the program PHASER in CCP4 [19] using the X-ray structure of YFP (PDB ID: 1MYW) as a reference model. The structure models were manually built using the program COOT [20] in CCP4, and non-crystallographic symmetry restraint refinement was performed using REFMAC5 in CCP4. All figures showing the atomic coordinates were created with PyMOL [21] and LIGPLOT [22]. Data collection and refinement statistics are summarized in Table 1.

2.5. Imaging of the redox status in HeLa cells

Oba-Q and Re-Q proteins were expressed in HeLa cells using modified pEGFP-N1 (Addgene) as an expression vector, and Lipofectamine3000 (Life Technologies) as a transfection reagent. The plasmid coding the mitochondria localized Re-Qc, pEGFP-N1/MitRe-Qc, was created by appending the human cytochrome *c* oxidase subunit 8A leader sequence to the 5′ end of the Re-Qc coding gene. The localization of MitRe-Qc was confirmed using MitoTracker® Red CMXRos (Invitorogen). C-terminus-deleted TagBFP mutants (TagBFPΔC12) and mCherry mutants (mCherryΔC7) were amplified by PCR and introduced into pEGFP-N1/Re-Qy1 and pEGFP-N1/Oba-Qc, respectively, by a hot fusion method [23]. After expression of the desired indicator proteins, cells were imaged on a confocal microscopy system, AxioObserverZ1, with LSM780 (Carl Zeiss). As excited light sources, Ar458/488/514 nm laser (25 mW) was used for Oba-Qc, Re-Qy, mCherry-Oba-Qc, and TagBFP-Re-Qy. DPSS 561 nm laser (20 mW) was used for mCherry-Oba-Qc and MitoTracker. Diode 405 nm laser (25 mW) was used for TagBFP-Re-Qy.The intensity of the fluorescence image was then digitalized using the image analysis software ImageJ.

Table 1
Data collection and refinement statistics.

	ReQy1	ReQy1CS
Native data		
X-ray source	SPring-8 BL44XU	
Detector	MX-300HE	
Wavelength (Å)	0.90000	
Space group	*C*2	$P2_1$
Unit cell parameters		
a, b, c (Å)	76.6, 120.5, 115.0	59.2, 70.7, 65.2
β (°)	106.2	95.0
Resolution range (Å)	50.00–2.30 (2.34–2.30)	50.00–2.40 (2.44–2.40)
Total number of reflections	142,671	63,141
Number of unique reflections	43,945	20,231
Multiplicity	3.2 (3.1)	3.1 (3.0)
Completeness (%)	99.0(99.9)	95.8(97.5)
Mean *I*/sigma (*I*)	33.9 (6.4)	13.7(2.4)
R-merge (*I*) (%)	15.6 (45.7)	12.8(57.2)
Refinement		
Resolution range (Å)	50.00–2.30	50.00–2.40
Reflection used	41,814	19,126
R_{work} (%)	18.4	19.0
R_{free} (%)	22.9	24.8
Total number of atoms	5910	3896
Averaged B-factor (Å ^{2})	42.6	32.3
RMSD from ideal values		
Bond length (Å)	0.0167	0.0133
Bond angles (deg)	1.9323	1.8126
Ramachandran plot		
Residues in most favored region(%)	96.8	97.4
Residues in allowed (%)	2.7	2.2
Residues in disallowed region (%)	0.5	0.4

The numerals in parentheses are for the highest resolution shell.

3. Results and discussion

3.1. Design of new redox-sensitive fluorescent protein sensors

To obtain the new redox sensor proteins, we adopted the molecular design of Oba-Qs and Oba-Qc from our previous study [15]: A cysteine pair, which can function as a switch reacting to the environmental redox state, was introduced at positions 147 and 204 of GFP derivatives. A single mutation at position 146 and a single amino acid insertion at the C-terminal side of Cys^{147} to enhance fluorescence intensity change were also introduced. We then introduced similar mutations into mTurquoise and Venus, and successfully obtained several redox sensor proteins. Some of these mutant proteins incidentally showed the reverse change in fluorescence from Oba-Q, implying quenching under reduced conditions. We therefore named them Re-Q proteins (reduction-sensed quenching proteins). Hereafter, $mTurquois_{F46L/Y145G/I146W/S147CG/Q204C}$ is referred to as Re-Qc, $Venus_{L71V/Y145G/N146W/S147CA/Q204C}$ as Re-Qy1, $Venus_{L71V/Y145G/N146W/S147CV/Q204C}$ as Re-Qy2, $mTurquois_{F46L/Y145G/I146G/S147CA/Q204C}$ as Oba-Qc2, and $mTurquois_{F46L/Y145G/I146G/S147CS/Q204C}$ as Oba-Qc3, as shown in Table 2.

Table 2
Summary of the redox-sensitive fluorescent proteins.

Name	Base	Mutation	Excitation (nm)	Emission (nm)	F_{ox}/F_{red}	Redox potential (mV)
Re-Qc	mTurquois	F46 L/Y145G/I146W/S147CG/Q204C	430	480	1.9	−286
Re-Qy1	Venus	L71 V/Y145G/N146 W/S147CA/Q204C	515	525	8.1	−263
Re-Qy2	Venus	L71 V/Y145G/N146 W/S147CV/Q204C	512	525	10.3	−251
Oba-Qc2	mTurquois	F46 L/Y145G/I146G/S147CA/Q204C	430	480	0.41	−267
Oba-Qc3	mTurquois	F46 L/Y145G/I146G/S147CS/Q204C	430	480	0.41	−259

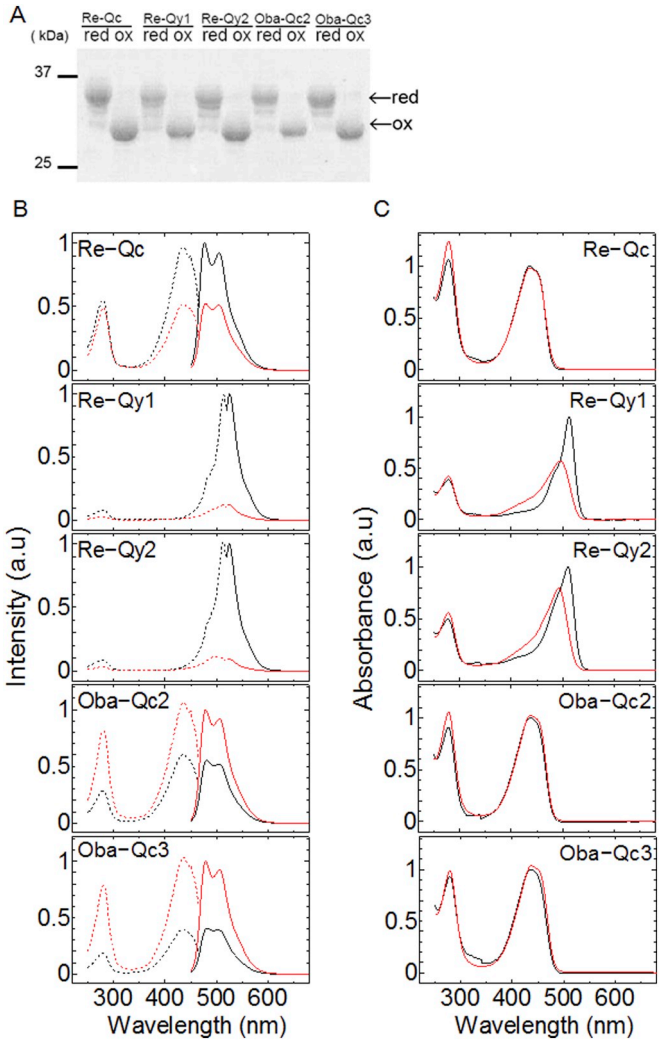

Fig. 1. Spectrophotometric properties of Oba-Q proteins. (A) Oxidation and reduction of Oba-Q and Re-Q proteins were confirmed by non-reducing SDS-PAGE followed by AMS labeling. For oxidation, the protein sample was treated with 1 mM diamide for 10 min, and for reduction incubated with 1 mM DTT for 10 min. (B) Excitation (dotted lines) and emission (solid lines) spectra of the oxidized (black lines) and reduced (red lines) forms of Re-Q and Oba-Q proteins. (C) Absorption spectra of the oxidized (black lines) and reduced (red lines) forms of Re-Q and Oba-Q proteins.

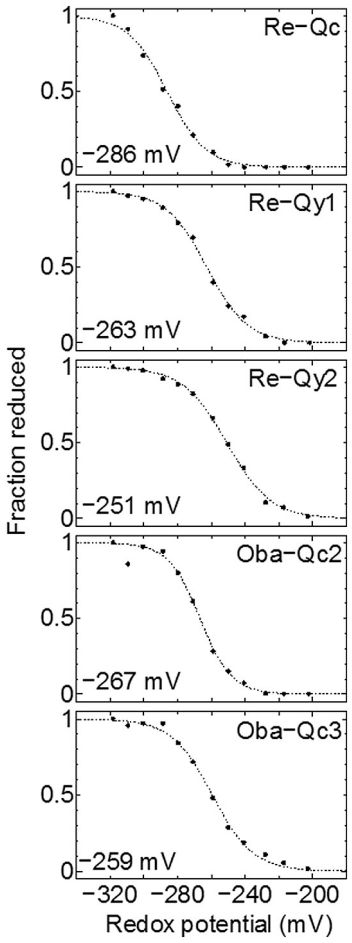

Fig. 2. Redox potentials of Re-Q and Oba-Q proteins. Redox potentials of Re-Q and Oba-Q proteins were determined at pH 7.0 by plotting the fraction of reduced protein, which was estimated from the fluorescence intensities, versus the ratio of DTTred to DTTox and fitting of the data on a titration curve.

3.2. Characterization of new redox-sensitive fluorescent proteins

Redox changes in cysteines of Re-Q and Oba-Q proteins were confirmed using the mobility shift on SDS-PAGE following AMS labeling of free thiols on the proteins [24] (Fig. 1A). Oba-Q and Re-Q mutants maintain the characteristic emission peaks of the chromophore of their parent proteins, CFP or YFP (Table 2). Oxidized forms of Re-Qc, Re-Qy1, and Re-Qy2 showed stronger fluorescence than those from the reduced-form proteins, and their fluorescence intensity ratio values between the oxidized form and reduced form (F_{ox}/F_{red}) were 1.9, 8.1, and 10.3, respectively (Fig. 1B and Table 2). In contrast, Oba-Qc2 and Oba-Qc3 showed stronger fluorescence intensities for the reduced forms (F_{red}) than for the oxidized forms (F_{ox}), and the resultant F_{ox}/F_{red} ratio values were 0.41 and 0.55, respectively (Fig. 1B and Table 2). The same as for the former Oba-Qc and Oba-Qs, the newly produced Re-Qc, Oba-Qc2, and Oba-Qc3 did not show remarkable changes in their absorption spectra (Fig. 1C) responding to the redox states of the protein molecules. The absorption peaks of the reduced forms of Re-Qy1 and Re-Qy2 differed from those of the oxidized forms (Fig. 1C), and these

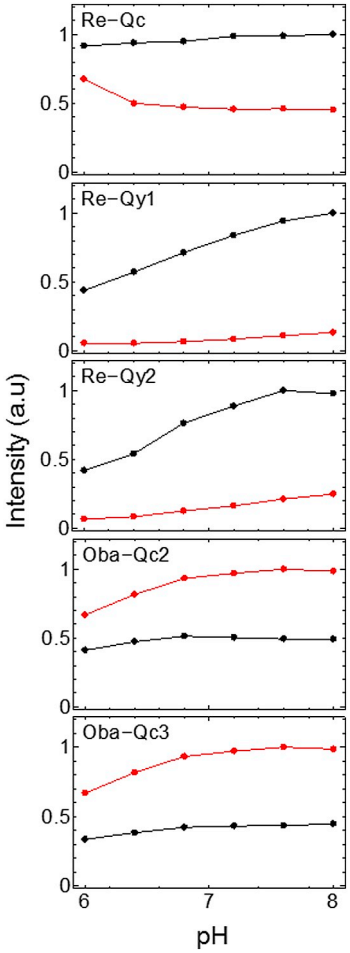

Fig. 3. pH dependence of Re-Q and Oba-Q proteins. Fluorescence levels from recombinant Re-Q and Oba-Q proteins at different pH were measured for their oxidized (black line) and reduced (red line) forms. Buffer: 100 mM Tris-HCl.

differences may have contributed to dramatic changes in the fluorescence intensity of these proteins.

We then determined the midpoint redox potentials of Re-Q and Oba-Q proteins from a plot of the fraction of reduced-form protein versus the ratio of DTT_{red} to DTT_{ox}, as described by Hanson et al. [9]. The results showed that these sensors could cover a wide range of the redox potentials in cells, from that in endoplasmic reticulum (ER) (estimated reduction potential $E_{pH\ 7} = -180$ mV) [25] to that in cytoplasm ($E_{pH\ 7} = -320$ mV) [16] of HeLa cells (Fig. 2, Table 2). The pH dependence of the fluorescence intensities of these sensor proteins was also examined (Fig. 3). The fluorescence intensities of the reduced and oxidized forms of CFP-based sensors, Re-Qc, Oba-Qc2, and Oba-Qc3, were mostly stable between pH 6.4 and pH 8.0, while YFP-based sensors, Re-Qy1 and ReQy2, were more susceptible to pH changes.

3.3. X-ray crystal structure analysis of Re-Qy1

To understand the molecular mechanism behind the quenching of the redox-sensitive fluorescence proteins shown in this study, we solved the crystal structures of the oxidized form and the reduced form of Re-Qy1 (Fig. 4A). Since disulfide bond formation on Re-Qy1 was observed even in the presence of the reductant under anaerobic conditions, it was extremely difficult to obtain structurally homogeneous samples of the reduced form of Re-Qy1 suitable for crystallization. We therefore prepared a Re-$Qy1_{SC}$ mutant whose redox-active cysteine residue, Cys^{147}, was replaced by serine to prevent undesirable disulfide bond formation. We compared absorbance, excitation and emission spectrum of Re-$Qy1_{SC}$ with those of oxidized and reduced forms of Re-Qy1, and confirmed that Re-$Qy1_{SC}$ showed same spectral characteristics with the reduced form Re-Qy1 (Fig. 4B and C). Consequently, the crystal structure of *Re*-Qy1 in the oxidized form and that of Re-$Qy1_{SC}$ in the mimic of the reduced form were solved at 2.0 Å (PDB ID: 6AA2) and 2.4 Å resolution (PDB ID: 6AA6), respectively. In both structures, the typical GFP backbone structures were conserved, whereas the main chain and side chain of the Trp^{146} residue showed dramatic structural changes according to the formation or dissociation of the disulfide bond on the molecule. In the oxidized form, a hydroxy group of the chromophore forms hydrogen bonds with His^{148} and Ser^{206} (Fig. 4C), whereas in the reduced form a peptide bond between Trp^{146} and Ser^{147} (equivalent to the redox-active Cys^{147} in Re-Qy1) of Re-$Qy1_{SC}$ residues has flipped, which leads to 180-degree rotation between the Cβ and Cγ atoms of Trp^{146}. Therefore, the Nε atom of rotated Trp^{146} sidechain in the reduced form can form an additional hydrogen bond to the hydroxy group at the tip of the chromophore (Fig. 4D). This new interaction only found in the reduced form must induce positional shifting of the chromophore by 1.3 Å and relocation of the chromophore against the sidechain of the Tyr^{203} residue, which results in cancellation of the π-π stacking between the chromophore and Tyr^{203} sidechain. Because the π-π stacking interaction is supposed to have important roles for the fluorescence of YFP, such as a red shift of the absorption peak and the facilitation of chromophore ionization, the cancellation of π-π stacking caused by the movement of the Trp^{146} residue must be the structural reason why the fluorescence of Re-Qy1 is quenched in the reduced form. In addition, dynamic structural change of backbone with the disulfide bond might influence the quantum yield of Re-Qy1 through changes in solvent accessibility or collision quenching. In the case of Re-Qc, these changes caused by the change in redox status might be reflected to the emission intensity of the protein.

3.4. Intracellular redox imaging

Next, we introduced Re-Q mutants into HeLa cells to investigate whether Re-Q mutants can detect the redox changes in vivo. When Re-Qy1 was expressed in the cytosol of HeLa cells, only a faint fluorescence image was observed under the fluorescence microscope, implying that the majority of the expressed Re-Qy1 was in the reduced form in the cell under standard culture conditions (Fig. 5, left panels). In contrast, when Re-Qc was introduced, it was in the half-oxidized forms under standard culture conditions, as judged from the fluorescence intensities under the fluorescence microscope (Fig. 5, right panels). These differences must have been caused by the difference of the midpoint redox potentials of these two sensor proteins, since the midpoint redox potential of Re-Qc is lower than that of Re-Qy1 (Table 2). Both Re-Q mutants expressed in the cells showed fluorescence when oxidants, 0.5 mM diamide, were added to the culture medium, and the observed fluorescence was immediately quenched when reductants, 5 mM DTT, were supplied (Fig. 5). We therefore concluded that midpoint redox potential of Re-Qc is within the practical range for use to monitor the intracellular redox environment. In contrast, Re-Qy1 was not suitable for the observation under standard culture conditions. This sensor must be more useful under oxidative stress conditions because Re-Qy1 showed a wide dynamic range at a higher redox potential range than other proteins. Hence, we can choose an appropriate sensor suitable for the particular subject of observation.

To demonstrate that Re-Q and Oba-Q mutants are applicable for the

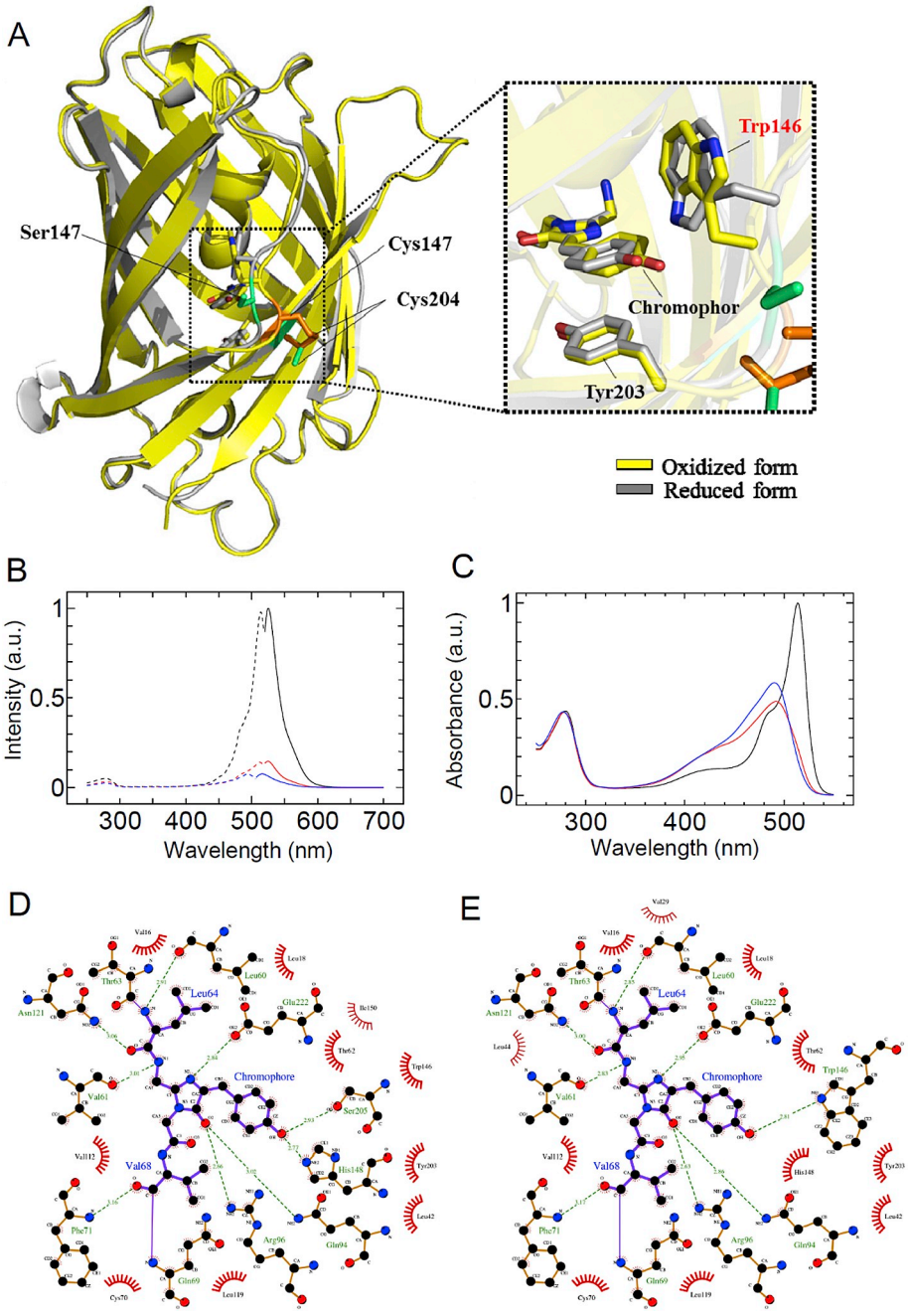

Fig. 4. X-ray crystal structures of Re-Qy1 and Re-Qy1$_{SC}$. (A) A ribbon diagram of Re-Qy1 (yellow) and Re-Qy1$_{CS}$ (gray). Both structures are shown as a superimposed model based on the main chain. (B) Excitation (dotted lines) and emission (solid lines) spectra of the oxidized (black lines) and reduced (red lines) forms of Re-Q1 and Re-Qy1$_{SC}$ (blue lines). (C) Absorption spectra of the oxidized (black lines) and reduced (red lines) forms of Re-Qy1 and Re-Qy1SC (blue lines). (D) Schematic illustration of interactions around the chromophore of Re-Qy1 in the oxidized form. (E) Schematic illustration of interactions around the chromophore in Re-Qy1$_{CS}$ in the reduced mimic form. (For interpretation of the references to color in this figure legend, the reader is referred to the web version of this article.)

multicolor observation of intracellular phenomena caused by oxidative stress, we expressed Re-Qy1 and Re-Qc in cytoplasm and mitochondria of cultured HeLa cells, respectively, and observed intracellular changes of the redox state in these compartments simultaneously (Fig. 6A). The cells were exposed to oxidative stress caused by Kp372–1, and the real-time changes of fluorescence were observed under a confocal fluorescent microscope. Kp372–1 is known as an inhibitor of PI3K/AKT/mTOR signaling pathways [26], and it is also known to be reduced by the overexpression of NAD(P)H dehydrogenase, which induces vigorous ROS generation in tumor cells [27]. In this study, we applied Kp372–1 as ROS inducer and tried to detect the intracellular oxidation caused by Kp372–1. When the cell was exposed to various concentrations of Kp372–1 for 5 min, oxidation of Re-Q proteins was observed (Fig. 6B). To determine the fluorescence intensity values under fully oxidized and fully reduced conditions, 1 mM diamide and 5 mM DTT were supplied to the cell culture, respectively, and the cell images were monitored. The oxidation ratios shown in Fig. 6C and D were calculated by the following equation:

$$Oxidation\ ratio = (F - F_{red})/(F_{ox} - F_{red}) \quad (9)$$

where F is the fluorescent intensity of Re-Q proteins at the indicated time, and F_{red} and F_{ox} are fluorescent intensities in fully reduced and

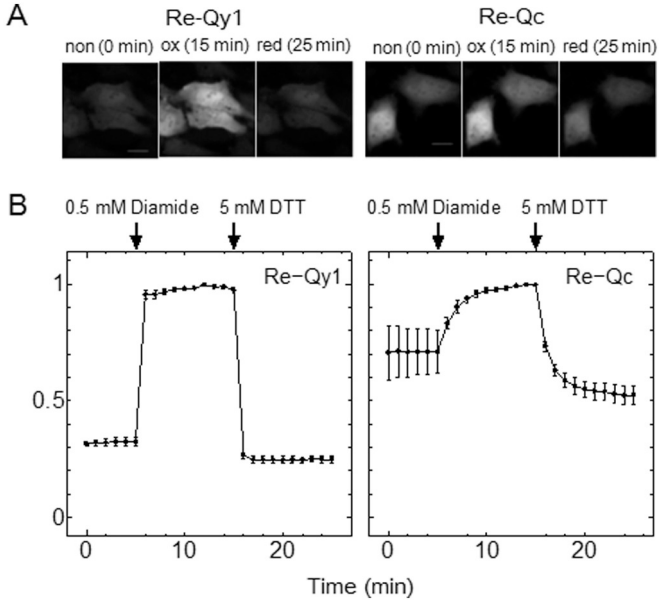

Fig. 5. Fluorescence redox responses of Re-Q proteins in living cells. HeLa cells expressing Re-Q proteins were observed under a confocal fluorescence microscope. (A) The images of the cells before the addition of diamide are shown for time 0 (0 min). Diamide at 0.5 mM was added at 5 min; 5 mM DTT was added at 15 min. Fluorescence images of the cells at the indicated time are presented. Scale bar, 20 μm. (B) Relative intensities of emission from images of 8 cells for Re-Qc and images of 12 cells for Re-Qy1 were averaged at the indicated time. Arrows indicate the times at which 0.5 mM diamide and 5 mM DTT were added.

fully oxidized conditions, respectively.

Tumor cells maintain their intracellular redox homeostasis by enhancing the glycolytic pathway, when they are exposed to oxidative stress [28]. Contributions of the glycolytic pathway to antioxidant stress were clearly visualized using Re-Qy1 and Re-Qc: When 0.1 μM Kp372-1 was added to the cell (Fig. 6C, D, and E, open arrow), the temporal oxidation of Re-Qy1 in the cytoplasm followed by its reduction was observed (Fig. 6C). We assumed that this reduction was caused by induction of the glycolytic pathway. We therefore supplied 20 μM heptelidic acid (HA), a selective inhibitor of GAPDH, together with Kp372–1, and observed remarkable oxidation (Fig. 6C, closed circle). In contrast, re-reduction was not observed in the cytosol (Fig. 6D, open circle) and the oxidation was accentuated when the glycolytic pathway was inhibited. Unexpectedly, HA itself also had an impact on oxidation in mitochondria (Fig. 6D). This might be caused by the indirect influence of cytosol oxidation.

3.5. Quantitative measurement using Re-Q and Oba-Q

As shown in Figs. 5 and 6, intracellular redox changes were easily visualized under the fluorescent microscope because of the remarkable single-wavelength fluorescence intensity changes of Re-Q or Oba-Q mutants. However, the signal from these sensors must be directly influenced by the amount of expressed sensor proteins in the cell, and it is therefore difficult to assess the redox changes in different cells. To overcome this problem, we prepared a fusion protein composed of these sensors with a redox-independent fluorescent protein such as TagBFP or mCherry (Fig. 7A). TagBFP-fused Re-Qy1 (TagBFP-Re-Qy1) and mCherry-fused Oba-Qc (mCherry-Oba-Qc) were then expressed in cytoplasm and ER of cultured HeLa cells respectively, followed by cell population analysis. Because the midpoint redox potential of Oba-Qc (−248 mV: pH 7.0) [15] is higher than that of Re-Qy1 (−263 mV: pH 7.0), Oba-Qc is thought to be more suitable for the observation under oxidized conditions such as in ER. When the fluorescence intensities of TagBFP and mCherry were used as reference values, the signal intensity peaks from Re-Qy1 and Oba-Qc clearly changed in a redox-dependent manner, while not being influenced by the expression levels of the sensor proteins (Fig. 7B and C).

Accordingly, marked oxidation in cytoplasm was observed when 2.5 μM Kp372–1 was added to the cell (Fig. 7B). To induce the redox change in ER, we applied thapsigargin (TG), which is known as an irreversible ER Ca^{2+}-ATPase inhibitor. When TG was added to the cell, Ca^{2+} in ER was depleted and consequently the redox status in ER became more reduced [29]. As shown in Fig. 7C, the small but detectable change in fluorescent ratios of mCherry-Oba-Qc ($p < .01$, Student's *t*-test) corresponding to the reduction in ER was observed when 10 μM TG was added (Fig. 7C). These results indicate that the redox sensor proteins fused with other fluorescent proteins are applicable for measuring intracellular redox changes.

4. Conclusion

We reported the new redox sensor proteins "Re-Q" derived from YFP or CFP. We previously reported the redox sensor proteins Oba-Q; however, they have a disadvantage for the practical use because their midpoint redox potentials are rather high to be used in reducing compartments in the cell such as cytoplasm and mitochondria of HeLa cells. By the introduction of several additional mutations, we could newly prepare the Oba-Q and Re-Q mutant proteins with significantly different midpoint redox potentials. This series of multicolor sensors covers wide range of redox potential, and must help visualization of the redox status of various cell compartments under various stress conditions.

Re-Q variants would be more suitable than Oba-Q for the redox biology research, because cells are generally kept under rather reducing conditions and oxidative stresses, rather than reductive stresses, are of more interest in the field. Because Re-Q emits fluorescence under the oxidative conditions, whereas Oba-Q gets quenched when oxidized, fluorescence signal from Re-Q gives higher signal-to-noise ratio than that from Oba-Q under physiological conditions. In addition, emission- and excitation-wavelengths of Re-Q variants hardly interfere with each other. By introducing these variants to different cell compartments, we can observe redox states in the different compartments of living cells simultaneously. Such multi-compartment redox imaging was not possible with previous redox sensor proteins such as roGFP.

Re-Q and Oba-Q proteins show single emission and excitation peaks, and this property might be the disadvantage for quantitative analysis; they are not applicable to the ratio-metric imaging and their fluorescent intensities are influenced by their expression levels. This problem is, however, solved by fussing Re-Q or Oba-Q sensor with non-redox sensitive fluorescent protein as shown in Fig. 7. In addition, we already succeeded to control the expression level of these sensor proteins in the cell compartments by fussing them with the endogenous protein whose expression level is also controlled in the cell [30,31].

In conclusion, newly developed Re-Q has a remarkable feature as a redox sensor protein in that Re-Q emits fluorescence when oxidized. Because of this feature and its color variations, Re-Q will shed light to unanswered questions on cellular redox responses, such as organelle-specific redox regulations.

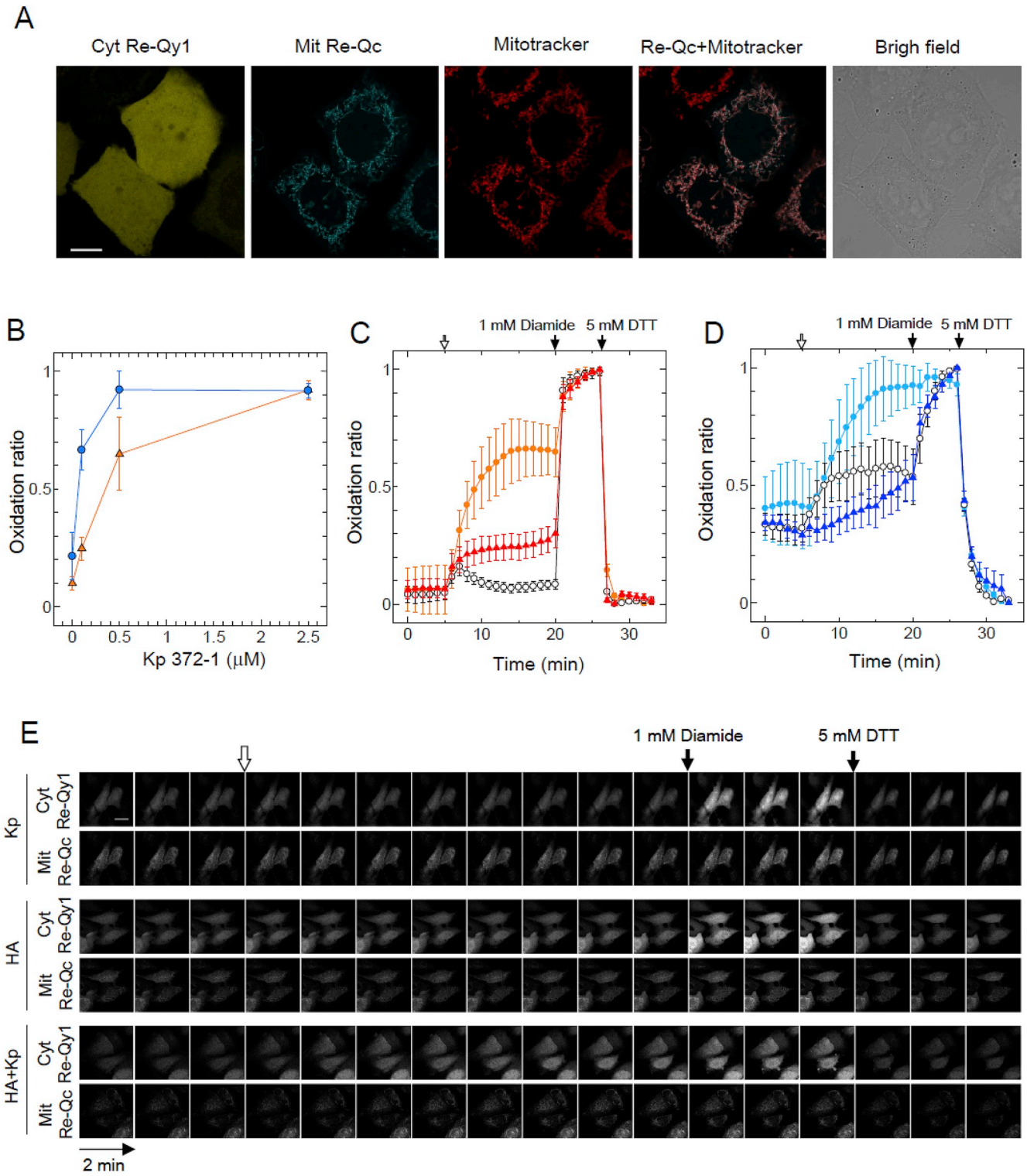

Fig. 6. Twin-color redox observation in living cells. (A) Re-Qc and Re-Qy1 were co-expressed in mitochondria and cytoplasm of HeLa cells. Cells were first treated with 0.5 mM diamide for 5 min. (B) Dependence of intracellular redox changes on Kp372–1 concentration. Oxidation ratios of Re-Qy expressed in cytosol (triangle) and Re-Qc expressed in mitochondria (closed circle) were measured 5 min after the addition of each concentration of Kp372–1 (*C–E*). Cells expressing these proteins were observed under a confocal fluorescence microscope. Oxidation ratios of Re-Qy expressed in cytosol (*C*) and Re-Qc in mitochondria (*D*) before the addition of reagent are shown for time 0 (0 min). Here 0.1 μM Kp372–1 (open circle), 20 μM HA (triangle), or both (closed circle) were added at 5 min (indicated as white arrows). Moreover, 1 mM diamide and 5 mM DTT were added at 20 and 26 min, respectively (black arrows). Oxidation ratio of Re-Qy and Re-Qc from images of 10 cells were averaged at the indicated time. Arrows indicate the times at which reagent was added. (*E*) Typical original images calculated for (*C*) and (*D*) are shown for every 2-min interval.

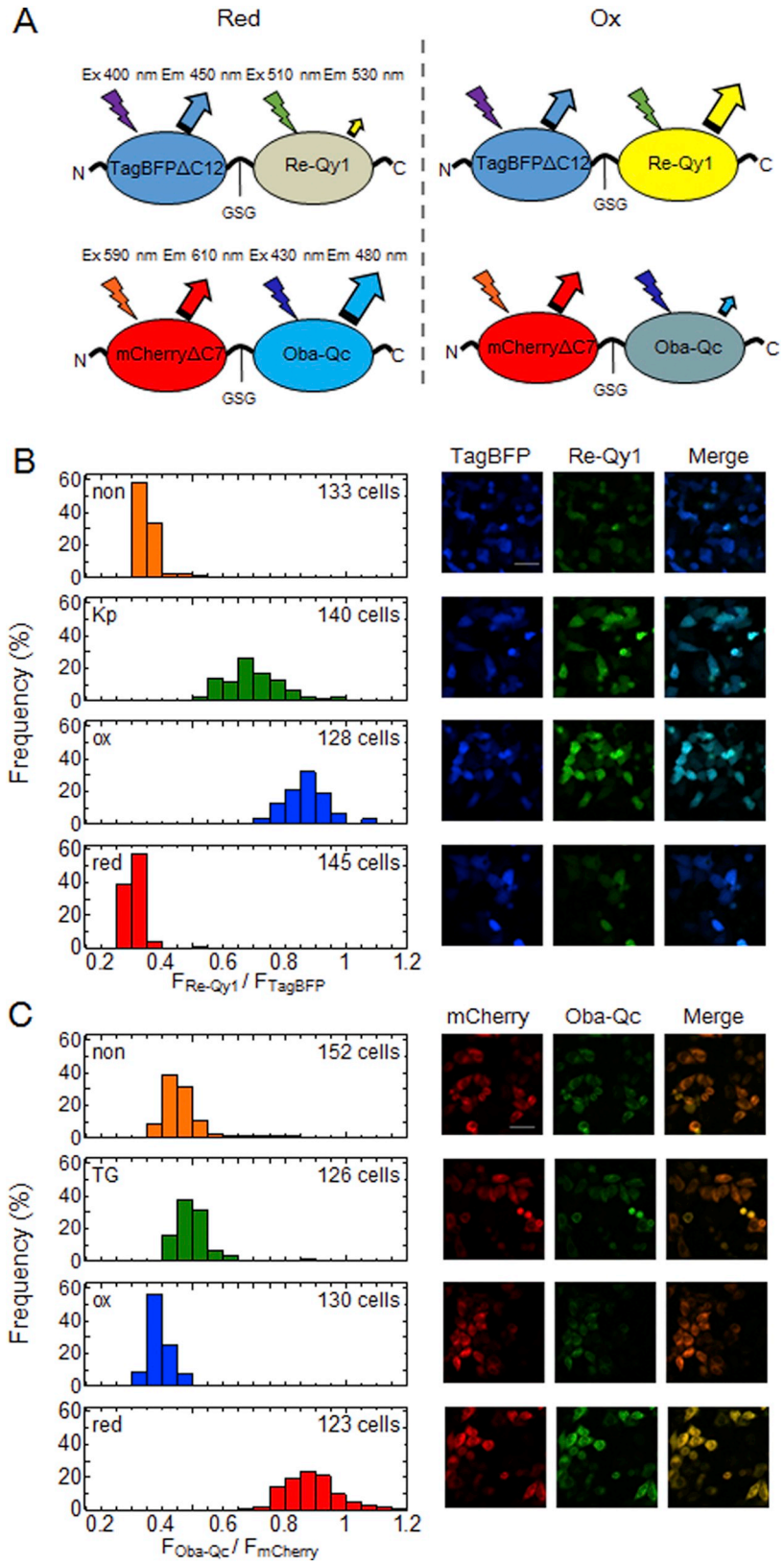

Fig. 7. Fluorescence redox responses of TagBFP-Re-Qy1 and mCherry-Oba-Qc in living cells. HeLa cells expressing fusion proteins were observed under a confocal fluorescence microscope. (A) Conceptual diagram of fusion sensors. (B, C) HeLa cells expressing TagBFP-Re-Qy1 in cytoplasm (B) or mCherry-Oba-Qc in ER(C) were observed under a confocal fluorescence microscope before (non) and after the addition of 2.5 μM Kp372–1 (Kp), 10 μM thapsigargin (TG), 0.5 mM diamide (ox) or 5 mM DTT (red). Fluorescence images are presented (right). Scale bar, 50 μm. Intensity ratios of emission from each cell type are displayed as histograms (left).

Acknowledgments

We thank Nami Tabushi, Aya Yasuda, and Atsuki Kawai for technical help with this project; Eiki Yamashita and A. Nakagawa for their support during X-ray data collection; Center for Biological Resources and Informatics and Suzukakedai Design and Manufacturing Division of Tokyo Institute of Technology for technical suports.

Declarations of interest

The authors declare that they have no conflicts of interest with the contents of this article.

Funding

This work was supported by JSPS KAKENHI Grant Number 16H06556 to T.H. and G. K., and by Dynamic Alliance for Open Innovation Bridging Human, Environment and Materials.

Author contributions

KS and TH conceived the study, and KS, HT and GK performed the experiments. KW and TH supervised the research. KS, GK, KW, and TH discussed the data. KS, GK and TH wrote the paper, and KW commented on the manuscript.

References

[1] B. Halliwell, Reactive species and antioxidants. Redox biology is a fundamental theme of aerobic life, Plant Physiol. 141 (2006) 312–322.
[2] F.Q. Schafer, G.R. Buettner, Redox environment of the cell as viewed through the redox state of the glutathione disulfide/glutathione couple, Free Radic. Biol. Med. 30 (2001) 1191–1212.
[3] E. Hideg, C. Barta, T. Kalai, I. Vass, K. Hideg, K. Asada, Detection of singlet oxygen and superoxide with fluorescent sensors in leaves under stress by photoinhibition or UV radiation, Plant Cell Physiol. 43 (2002) 1154–1164.
[4] B.B. Buchanan, Role of light in the regulation of chloroplast enzymes, Annual Review of Plant Physiology and Plant Molecular Biology, vol. 31, 1980, pp. 341–374.
[5] S.W. Kang, I.C. Baines, S.G. Rhee, Characterization of a mammalian peroxiredoxin that contains one conserved cysteine, J. Biol. Chem. 273 (1998) 6303–6311.
[6] M. Baier, K.J. Dietz, The plant 2-Cys peroxiredoxin BAS1 is a nuclear-encoded chloroplast protein: its expressional regulation, phylogenetic origin, and implications for its specific physiological function in plants, Plant J. 12 (1997) 179–190.
[7] R. Scheibe, J.E. Backhausen, V. Emmerlich, S. Holtgrefe, Strategies to maintain redox homeostasis during photosynthesis under changing conditions, J. Exp. Bot. 56 (2005) 1481–1489.
[8] C.H. Foyer, G. Noctor, Redox homeostasis and antioxidant signaling: a metabolic interface between stress perception and physiological responses, Plant Cell 17 (2005) 1866–1875.
[9] G.T. Hanson, R. Aggeler, D. Oglesbee, M. Cannon, R.A. Capaldi, R.Y. Tsien, S.J. Remington, Investigating mitochondrial redox potential with redox-sensitive green fluorescent protein indicators, J. Biol. Chem. 279 (2004) 13044–13053.
[10] H. Ostergaard, A. Henriksen, F.G. Hansen, J.R. Winther, Shedding light on disulfide bond formation: engineering a redox switch in green fluorescent protein, EMBO J. 20 (2001) 5853–5862.
[11] T. Yano, M. Oku, N. Akeyama, A. Itoyama, H. Yurimoto, S. Kuge, Y. Fujiki, Y. Sakai, A novel fluorescent sensor protein for visualization of redox states in the cytoplasm and in peroxisomes, Mol. Cell. Biol. 30 (2010) 3758–3766.
[12] Y. Fan, Z. Chen, H.W. Ai, Monitoring redox dynamics in living cells with a redox-sensitive red fluorescent protein, Anal. Chem. 87 (2015) 2802–2810.
[13] J.R. Lohman, S.J. Remington, Development of a family of redox-sensitive green fluorescent protein indicators for use in relatively oxidizing subcellular environments, Biochemistry. 47 (2008) 8678–8688.
[14] W. Tomosugi, T. Matsuda, T. Tani, T. Nemoto, I. Kotera, K. Saito, K. Horikawa, T. Nagai, An ultramarine fluorescent protein with increased photostability and pH insensitivity, Nat. Methods 6 (2009) 351–353.
[15] K. Sugiura, T. Nagai, M. Nakano, H. Ichinose, T. Nakabayashi, N. Ohta, T. Hisabori, Redox sensor proteins for highly sensitive direct imaging of intracellular redox state, Biochem. Biophys. Res. Commun. 457 (2015) 242–248.
[16] C.T. Dooley, T.M. Dore, G.T. Hanson, W.C. Jackson, S.J. Remington, R.Y. Tsien, Imaging dynamic redox changes in mammalian cells with green fluorescent protein indicators, J. Biol. Chem. 279 (2004) 22284–22293.
[17] W.W. Cleland, Dithiothreitol, a new protective reagent for Sh groups, Biochemistry 3 (1964) 480–482.
[18] Z. Otwinowski, W. Minor, Processing of X-ray diffraction data collected in oscillation mode, Methods Enzymol. 276 (1997) 307–326.
[19] N. Collaborative Computational Project, The CCP4 suite: programs for protein crystallography, Acta Crystallogr. D Biol. Crystallogr. 50 (1994) 760–763.
[20] P. Emsley, K. Cowtan, Coot: model-building tools for molecular graphics, Acta Crystallogr. D Biol. Crystallogr. 60 (2004) 2126–2132.
[21] L. Schrodinger, The PyMOL Molecular Graphics System, (2010) Version 1.3r1 (eds.).
[22] A.C. Wallace, R.A. Laskowski, J.M. Thornton, LIGPLOT: a program to generate schematic diagrams of protein-ligand interactions, Protein Eng. 8 (1995) 127–134.
[23] C. Fu, W.P. Donovan, O. Shikapwashya-Hasser, X. Ye, R.H. Cole, Hot fusion: an efficient method to clone multiple DNA fragments as well as inverted repeats without ligase, PLoS One 9 (2014) e115318.
[24] T. Kobayashi, S. Kishigami, M. Sone, H. Inokuchi, T. Mogi, K. Ito, Respiratory chain is required to maintain oxidized states of the DsbA-DsbB disulfide bond formation system in aerobically growing Escherichia coli cells, Proc. Natl. Acad. Sci. U. S. A. 94 (1997) 11857–11862.
[25] C. Hwang, A.J. Sinskey, H.F. Lodish, Oxidized redox state of glutathione in the endoplasmic reticulum, Science. 257 (1992) 1496–1502.
[26] M. Mandal, S. Kim, M.N. Younes, S.A. Jasser, A.K. El-Naggar, G.B. Mills, J.N. Myers, The Akt inhibitor KP372-1 suppresses Akt activity and cell proliferation and induces apoptosis in thyroid cancer cells, Br. J. Cancer 92 (2005) 1899–1905.
[27] Y. Zhao, Q. Hu, F. Cheng, N. Su, A. Wang, Y. Zou, H. Hu, X. Chen, H.M. Zhou, X. Huang, K. Yang, Q. Zhu, X. Wang, J. Yi, L. Zhu, X. Qian, L. Chen, Y. Tang, J. Loscalzo, Y. Yang, SoNar, a highly responsive NAD+/NADH sensor, allows high-throughput metabolic screening of anti-tumor agents, Cell Metab. 21 (2015) 777–789.
[28] C. Cerella, M. D'Alessio, S. Cristofanon, M. De Nicola, F. Radogna, M. Dicato, M. Diederich, L. Ghibelli, Subapoptogenic oxidative stress strongly increases the activity of the glycolytic key enzyme glyceraldehyde 3-phosphate dehydrogenase, Ann. N. Y. Acad. Sci. 1171 (2009) 583–590.
[29] E. Avezov, B.C. Cross, G.S. Kaminski Schierle, M. Winters, H.P. Harding, E.P. Melo, C.F. Kaminski, D. Ron, Lifetime imaging of a fluorescent protein sensor reveals surprising stability of ER thiol redox, J. Cell Biol. 201 (2013) 337–349.
[30] K. Sugiura, Y. Nishimaki, M. Owa, T. Hisabori, K.I. Wakabayashi, Assessment of the flagellar redox potential in Chlamydomonas reinhardtii using a redox-sensitive fluorescent protein, Oba-qc, Biochem. Biophys. Res. Commun. 503 (2018) 2083–2088.
[31] M. Owa, A. Furuta, J. Usukura, F. Arisaka, S.M. King, G.B. Witman, R. Kamiya, K. Wakabayashi, Cooperative binding of the outer arm-docking complex underlies the regular arrangement of outer arm dynein in the axoneme, Proc. Natl. Acad. Sci. U. S. A. 111 (2014) 9461–9466.